GEOPHYSICAL RESEARCH LETTERS, VOL. 24, NO. 23, PAGES 3073-3076, DECEMBER 1, 1997

Global Positioning System constraints on fault slip rates in the Death Valley region, California and Nevada

R. A. Bennett[1], B. P. Wernicke[2], J. L. Davis[1], P. Elósegui[1,3], J. K. Snow[2], M. J. Abolins[2], M. A. House[2], G. L. Stirewalt[4], and D. A. Ferrill[4]

Abstract. We estimated horizontal velocities at 15 locations in the vicinity of Yucca Mountain, Nevada, from Global Positioning System surveys conducted between 1991 and 1996. We used these velocity estimates to infer slip rates on two major Quaternary faults within the eastern California shear zone (ECSZ), the Hunter Mountain and Death Valley faults. The sum of slip rates across the two faults is well determined at 5 ± 1 mm/yr (1-σ). Between 3 to 5 mm/yr of this motion appears to be accommodated along the Death Valley fault, implying 30–50 m of strain accumulation over the next 10,000 yr. If so, there is potential for 5 to 10 M_w 6.5–7.5 earthquakes during this period, a finding consistent with paleoseismological studies of the fault zone. Yucca Mountain, which lies 50 km east of the ECSZ, is the proposed location for the disposal of high-level nuclear waste in the United States.

Introduction

Between 9% and 23% of modern Pacific-North America relative plate motion is transferred from the Salton Trough of southern California to the Basin and Range Province of the western United States by means of the eastern California shear zone (ECSZ) [*Sauber et al.*, 1994] (Figure 1). The contemporary distribution of deformation within the ECSZ has important implications for the long term accumulation and release of strain in the continental crust and bears directly on the reliability of paleoseismological inferences for assessing seismic risk. Although much has been learned about the ECSZ through geological observations and conventional terrestrial and space geodetic measurements, the distribution of strain accumulation at latitude ~37°N is not yet well constrained. A better understanding of this deformation is critical, as Yucca Mountain, Nevada, the proposed disposal site for high-level nuclear waste in the United States, lies only 50 km to the east.

At latitude 37°N, the ECSZ is expressed mainly as three right-lateral, locally transtensional fault zones: the Death Valley-Furnace Creek (DVFC), Hunter Mountain-Panamint Valley (HMPV), and Owens Valley (OVFZ) fault zones (Figure 1). Geological evidence indicates that since 5 Ma the ECSZ accommodated ~10 mm/yr of right-lateral displacement across these faults [e.g., *Wernicke et al.*, 1988]. Paleoseismological data, representing Quaternary strain release, indicate that the DVFC fault zone and its northern extension, the Fish Lake Valley fault zone, accommodated 4–6 mm/yr or more of right-lateral motion [*Brogen et al.*, 1991; *Reheis and Sawyer*, 1997]. Somewhat smaller slip rates are estimated for the HMPV fault zone (2.4 ± 0.8 mm/yr) [*Zhang et al.*, 1990] and for the OVFZ and its northern extension, the White Mountain fault zone (0.5–2.0 mm/yr) [*dePolo*, 1989; *Beanland and Clark*, 1995].

At latitude 34.5°N, the ECSZ manifests itself within Mojave Desert terrestrial geodetic networks as an apparent right-lateral northwest shear of as much as 12 mm/yr extending northward into Owens Valley [*Sauber et al.*, 1994]. Deformation within these networks attenuates rapidly eastward. At latitude 37°N, there is no evidence for deformation greater than about 2 mm/yr across the Yucca Mountain trilateration network [*Savage et al.*, 1994]. Deformation within the Owens Valley trilateration network to the west accounts for up to 7 mm/yr of right-lateral slip on the OVFZ fault [*Savage and Lisowski*, 1995]. These results suggest that present-day strain accumulation at 37°N may be concentrated along the western margin of the ECSZ, in contrast to the paleoseismological data which indicate concentration of strain toward the east. Several models have been formulated to reconcile the discrepancy between these observations, all involving westward migration of shear strain within the ECSZ over the last few million years [e.g., *Dokka and Travis*, 1990; *Savage and Lisowski, 1995*; *Dixon et al.*, 1995].

In this paper we use Global Positioning System (GPS) observations collected over the last five years to investigate the distribution and sum of contemporary deformation along the portion of the ECSZ east of Owens Valley and in the vicinity of Yucca Mountain. We reserve a detailed discussion of deformation in the direct vicinity of Yucca Mountain for a future publication.

GPS Observations

Between 1991 and 1996, we conducted five GPS surveys within and around the ECSZ in the vicinity of Yucca Mountain, Nevada. The network consisted of 15 stations comprising three subnetworks and two additional sites (Figures 1 and 2). We analyzed the GPS data using the GAMIT/GLOBK software [*King and Bock*, 1995; *Herring*, 1995]. In our analyses we included all available global tracking data from the International GPS Service for Geodynamics (IGS) and used data products provided by the Scripps Orbit and Permanent Array Center.

[1]Harvard-Smithsonian Center for Astrophysics, Cambridge, MA

[2]California Institute of Technology, Pasadena, CA

[3]Institut d'Estudis Especials de Catalunya, Barcelona, Spain

[4]Center for Nuclear Waste Regulatory Analyses, San Antonio, TX

Paper number 97GL02951.
0094-8534/97/97GL-02951$05.00

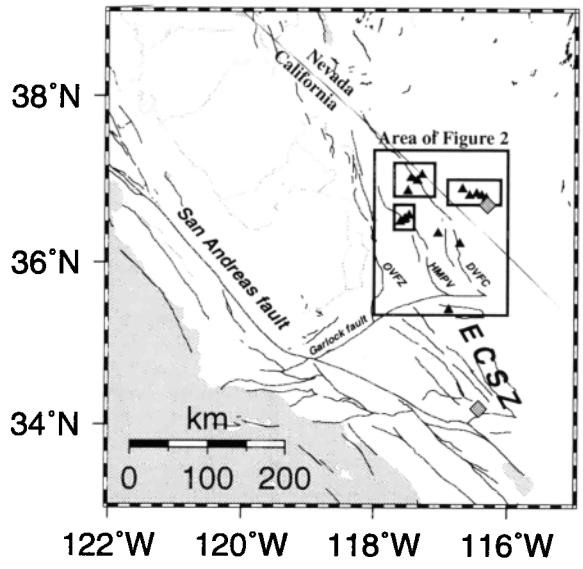

Figure 1. General location map. GPS sites indicated by black triangles. Small boxes show locations of subnetworks. Largest box shows the location of Figures 2 and 4. DVFC, HMPV, and OVFZ indicate locations of the Death Valley-Furnace Creek, Hunter Mountain-Panamint Valley, and Owens Valley fault zones. Diamonds show locations of the 1992 M_s 7.5 Landers (CA) and M_s 5.4 Little Skull Mountain (NV) earthquakes.

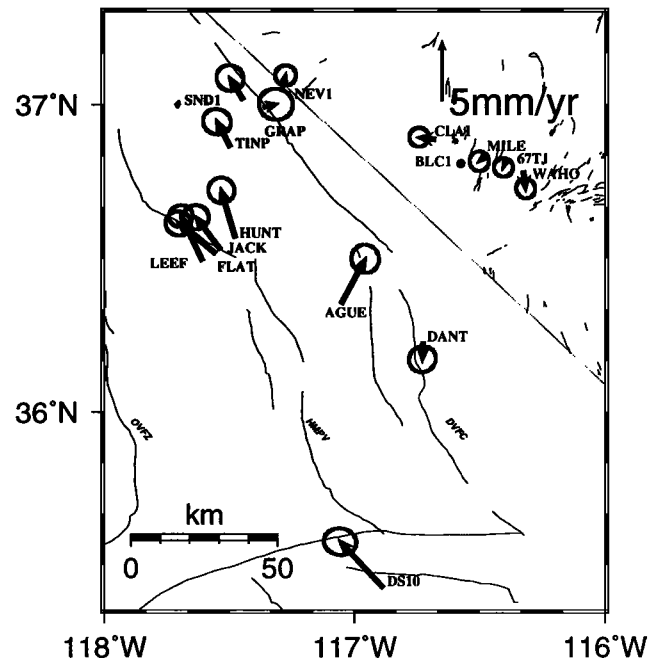

Figure 2. Velocity estimates from 1991–1996 GPS observations with respect to BLC1. Ellipses represent 95% confidence level. Dark sinuous lines represent faults; dashed northwest trending straight line represents the California-Nevada border.

We investigated the extent to which our velocity estimates were affected by coseismic displacements associated with the 1992 M_s 7.5 Landers and M_s 5.4 Little Skull Mountain earthquakes (Figure 1), and found that our data are not sensitive to these earthquakes due to the rather large uncertainties in the positions estimated from the 1991 survey.

We show our velocity estimates computed with respect to site BLC1 in Figure 2, and list these estimates in Table 1. Figure 3 shows the time evolution of the LEEF-BLC1 baseline. The average weighted root-mean-square scatters in the components of the residual baseline estimates (removing the trend derived from the rate estimates) are 2, 2, and 9 in the north, east, and up components, respectively. The corresponding χ^2 per degree of freedom values for all baseline components are near 1.0, indicating that the formal uncertainties are consistent with the scatter in the data. Vertical velocity estimates are significant at the 95% confidence level for three sites (DANT, GRAP, WAHO; Table 1).

From the horizontal velocity estimates we make the following observations: The total deformation across the network west of BLC1 (relative motion between sites BLC1 and LEEF) is 4.0 ± 0.5 mm/yr (1-σ). Deformation within the network is dominated by right-lateral northwest trending shear with steepest gradients over the DVFC fault zone. The exception to this general pattern is site AGUE which exhibits a large component of motion perpendicular to the average direction of shear. Deformation among sites in the Yucca Mountain subnetwork is small, consistent with the results of *Savage et al.* [1994].

Dislocation Model

We followed the modeling and inversion approach of *Bennett et al.* [1996] to eliminate the dependence of our modeling results on possible GPS reference frame biases. The portion of the ECSZ within the span of our network was modeled as a set of elastic blocks bounded by planar, infinite, parallel dislocations representing, from east to west, the DVFC, HMPV, and OVFZ fault zones (Figure 4). The faults were assumed to be locked to 15 km depth. Model velocities were computed from a superposition of relative, rigid body motions and the elastic deformation field induced by the locked, near surface parts of the faults. We constrained the azimuth of relative block motions to be equal to that of the dislocation planes (320°).

Table 1. GPS Site Velocities (mm/yr)

Site	Lon.	Lat.	East	North	Up
67TJ	243.6	36.8	-0.2 ± 0.3	-0.4 ± 0.3	-3 ± 2
AGUE	242.9	36.4	1.9 ± 0.5	3.6 ± 0.5	0 ± 3
BLC1	243.4	36.8	0.0 ± 0.0	0.0 ± 0.0	0 ± 0
CLAI	243.3	36.9	-1.2 ± 0.3	0.1 ± 0.3	-2 ± 2
DANT	243.3	36.2	0.0 ± 0.5	-1.4 ± 0.4	10 ± 3
FLAT	242.4	36.5	-3.0 ± 0.4	2.5 ± 0.4	-4 ± 3
GRAP	242.6	37.9	1.0 ± 0.6	0.3 ± 0.5	-9 ± 4
HUNT	242.5	36.6	-1.1 ± 0.4	3.8 ± 0.4	-4 ± 3
JACK	242.5	36.5	-2.0 ± 0.4	2.7 ± 0.4	-3 ± 3
LEEF	242.4	36.5	-1.8 ± 0.4	3.6 ± 0.4	0 ± 2
MILE	243.5	36.8	-0.7 ± 0.3	-0.5 ± 0.3	-4 ± 2
NEV1	242.7	37.1	0.2 ± 0.4	0.9 ± 0.3	-2 ± 2
SND1	242.6	37.0	-1.0 ± 0.5	1.7 ± 0.4	-2 ± 3
TINP	242.5	36.7	-1.0 ± 0.5	2.0 ± 0.4	-1 ± 3
WAHO	243.7	36.8	0.1 ± 0.3	-1.4 ± 0.3	-6 ± 2

Velocities relative to BLC1. Uncertainties are 1-σ.

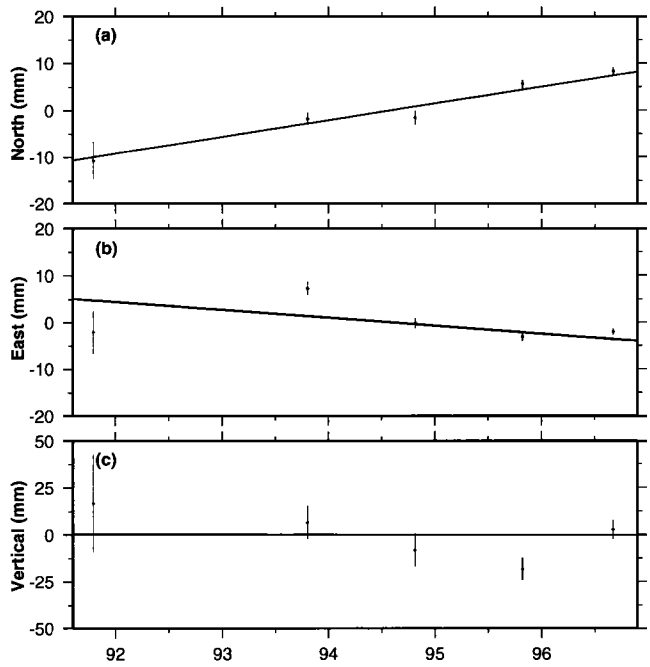

Figure 3. Time series of LEEF with respect to BLC1. Velocity estimates for baseline components are (a) north, 3.6 ± 0.4 mm/yr; (b) east, -1.8 ± 0.4 mm/yr; (c) up, 0 ± 2.

Using the horizontal components of our GPS velocity estimates and their error covariance matrix, we estimated slip rates on the three model faults. Because our model is one dimensional, we did not use the velocities at sites DANT and AGUE, as these sites lie close to a major right stepping jog in the DVFC fault zone. We achieved a χ^2 value of 124, yielding a χ^2 per degree of freedom of about 6. The resulting slip rate estimates are listed in Table 2 (solution 1).

As expected, the OVFZ slip rate is very poorly resolved (solution 1, Table 2). Therefore, we re-estimated the DVFC and HMPV slip rates in two solutions wherein the OVFZ fault slip rate was constrained to the values of 0 mm/yr and 7 mm/yr (solutions 2 and 3), respectively. We found that the estimates for the DVFC and HMPV slip rates are unaffected at the 1-σ level and that the increase in the χ^2 was insignificant for both cases. We performed a similar numerical experiment wherein the HMPV fault slip rate was constrained to zero (solution 4) with similar results. In this solution, the slip rate estimate for the DVFC fault accommodates all of the motion within the network; it is equal to the sum of the DVFC and HMPV slip rate estimates of the previous solutions. Finally, we estimated the HMPV and OVFZ slip rates under the hypothesis that the DVFC slip rate is zero (solution 5). We may reject this hypothesis given our data and model with greater than 98% confidence. We cannot reject with sufficient confidence models in which the slip rate on either the HMPV or OVFZ fault is constrained to be zero. The DVFC slip rate estimate resulting when both these slip rates are constrained to zero (solution 6) is large and well determined (5±1 mm/yr). The residual velocity field associated with this solution is shown in Figure 4.

We then tested the sensitivity of the velocity estimates to the locking depths of the DVFC and HMPV faults. We performed four additional solutions using the parameterization of solution 6 but with the locking depth of the DVFC fault set to 10, 13, 17 and 20 km. The resulting DVFC fault slip rate estimates are unchanged relative to the value of solution 6 to within their uncertainties. Geological evidence suggests that the locking depth of the HMPV fault zone may be very shallow [*Burchfiel et al.*, 1987]. Estimating the slip rates on all three fault systems, under the assumption of a 5 km locking depth for the HMPV fault, yields marginally smaller rates for all faults with slightly smaller uncertainties.

Because the fault traces are clearly not linear, we tested the sensitivity of our results to the value of the strike

Table 2. Fault Slip Rate Estimates (mm/yr)

No.	DVFC	HMPV	OVFZ	DV+HM	χ^2	SL
1	3 ± 2	3 ± 3	-8 ± 24	6 ± 2	124	-
2	3 ± 2	2 ± 3	0	5 ± 2	126	39%
3	4 ± 2	2 ± 3	7	5 ± 2	128	52%
4	5 ± 1	0	4 ± 20	5 ± 1	126	33%
5	0 ± 0	7 ± 2	-27 ± 24	7 ± 2	160	98%
6	5 ± 1	0	0	5 ± 1	126	0%
7	3 ± 1	2 ± 2	1 ± 2	5 ± 1	126	-

DVFC = Death Valley-Furnace Creek fault slip rate. HMPV = Hunter Mountain-Panamint Valley fault slip rate. OVFZ = Owens Valley fault slip rate. DV+HM = DVFC + HMPV. SL = significance level (see text). All rates estimated without a priori constraints except: (1) Those for which no standard error is shown are fixed to this value; and (2) Solution 7, HMPV and OVFZ constrained to their paleoseismological values (see text). Uncertainties are 1-σ.

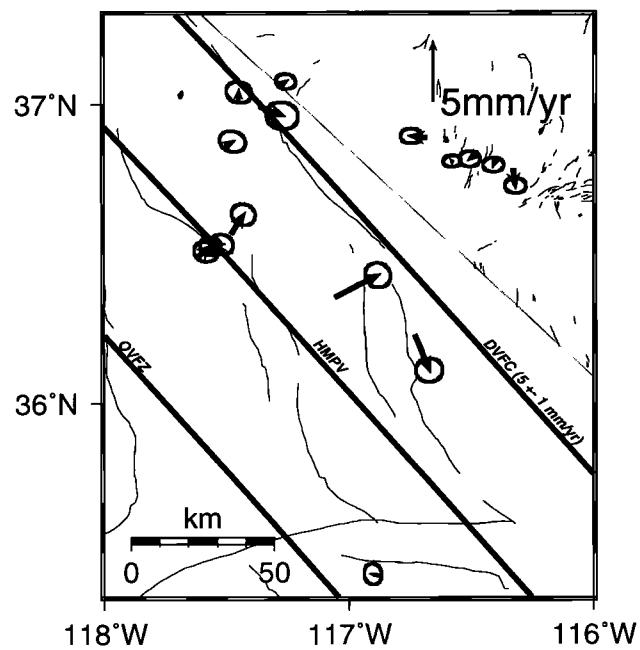

Figure 4. Residual velocities after removing model associated with solution 6 (Table 2). Model faults are indicated by dark solid lines. Ellipses represent 95% confidence level. AUGE, DANT, and DS10 were not used in determining the fault slip rate.

adopted. We found no significant variation in the results through the range 310–330°.

Finally, we tested a solution wherein we constrained the values of the OVFZ and HMPV fault slip rates to their paleoseismological estimates of 2.0 ± 0.5 and 2.4 ± 0.8 mm/yr, respectively [*Beanland and Clark,* 1995; *Zhang et al.,* 1990]. The estimate that we obtain for the DVFC fault of 3 ± 1 mm/yr (solution 7) differs insignificantly from the paleoseismological estimates of 4–6 mm/yr [e.g., *Reheis and Sawyer,* 1997].

Discussion and Conclusion

An additional measurement of the integrated deformation across our network resulted from our GPS analyses; we estimated a rate of 5.1 ± 0.7 mm/yr relative motion between sites DS10 (part of the IGS network) and BLC1 (Figure 2). DS10 lies well east of the southern extrapolation of the OVFZ fault zone, but west of the extrapolations of the HMPV and DVFC fault zones. Although the applicability of our simple model is questionable south of the Garlock fault, we found that the north and east components of the difference between our velocity estimate for site DS10 and the velocity predicted by our model are insignificant at 0.1 ± 0.4 and −0.3 ± 0.3 mm/yr, respectively (Figure 4).

We cannot distinguish between 0 and 7 mm/yr slip rate on the Owens Valley fault with our data set. Similarly, we provide only very loose constraints on the slip rate of the Hunter Mountain fault (σ = 3 mm/yr). However, our velocity field is consistent with paleoseismological estimates of slip rate within these fault zones and with other geodetic and geological observations. Within error, our slip rate estimates are consistent with rates suggested by *Dixon et al.* [1995]. Although evidence from previous studies discussed above suggests a general westward shift of deformation across the three fault zones in the region with time, our results suggest that substantial active shear (3–5 of the total 6–12 mm/yr) is concentrated on the eastern portion of the ECSZ.

Paleoseismological analyses of the Death Valley fault zone indicate that 4 to 6 separate moderate to large (M > 6.5) earthquakes have occurred along various segments of the fault since 10 ka [e.g., *Brogen et al.,* 1991]. Given the 3–5 mm/yr slip rate that we infer for the Death Valley fault, we may expect 5–10 M_W 6.5–7.5 earthquakes to occur over the next ten thousand years.

Acknowledgments. This work was supported by Nuclear Regulatory Commission (NRC) Contracts NRC-04-92-071 and NRC-02-93-005, NSF Grant EAR-94-18784, and the Smithsonian Institution. The views and conclusions expressed in this paper do not represent an official regulatory position of the United States NRC. This manuscript benefited from careful reviews by E. Humphreys, R. Snay, and an anonymous referee, and useful discussions with J. Savage. Figures were created with the GMT software.

References

Beanland, S. and M. M. Clark, The Owens Valley fault zone, eastern California, and surface rupture associated with the 1872 earthquake, *U.S. Geol. Sur. Bull., 1892,* 1995.

Bennett, R. A., W. Rodi, and R. E. Reilinger, Global Positioning System constraints on fault slip rates in southern California and northern Baja, Mexico, *J. Geophys. Res., 101,* 21,943–21,960, 1996.

Brogen, G. E., K. S. Kellog, D. B. Slemmons, and C. Terhune, Late Quaternary faulting along the Death Valley-Furnace Creek fault system, California and Nevada, *U.S. Geol. Surv. Bull., 1991,* 23 pp., 1991.

Burchfiel, B. C., K. V. Hodges, and L. H. Royden, Geology of Panamint Valley – Saline Valley pull-apart system, California: Palinspastic evidence for low-angle geometry of a Neogene range-bounding fault, *J. Geophys. Res., 91,* 10.422–10,426, 1987.

dePolo, C. M., *Seismotectonics of the White Mountains fault system, east-central California, and west-central Nevada,* PhD thesis, University of Nevada, Reno, 1989.

Dixon, T. H., R. Stefano, J. Lee, and M. C. Reheis, Constraints on present-day Basin and Range deformation from space geodesy, *Tectonics, 14,* 755–772, 1995.

Dokka, R. K. and C. J. Travis, Role of the eastern California shear zone in accommodating Pacific-North American plate motion, *Geophys. Res. Lett., 17,* 1323–1326, 1990.

Herring, T. A., GLOBK: Global Kalman filter VLBI and GPS analysis program, Dept. of Earth, Atmospheric, and Planetary Sciences, Massachusetts Institute of Technology, Cambridge, MA, 1995.

King, R. W. and Y. Bock, Documentation for the MIT GPS analysis software: GAMIT, Dept. of Earth, Atmospheric, and Planetary Sciences, Massachusetts Institute of Technology, Cambridge, MA, 1995.

Reheis, M. C. and T. L. Sawyer, Late Cenozoic history and slip rates of the Fish Lake Valley, Emigrant Peak, and Deep Springs fault zones, Nevada and California, *Geol. Soc Am. Bull., 109,* 280–299, 1997.

Sauber, J., W. Thatcher, S. Solomon, and M. Lisowski, Geodetic slip rate for the eastern California shear zone and the recurrence time of Mojave desert earthquakes, *Nature, 367,* 264–266, 1994.

Savage, J. C. and M. Lisowski, Strain accumulation in Owens Valley, California, *Bull. Seis. Soc. Am., 85,* 151–158, 1995.

Savage, J. C., M. Lisowski, W. K. Gross, N. E. King, and J. L. Svarc, Strain accumulation near Yucca Mountain, Nevada, 1983-1993, *J. Geophys. Res., 99,* 18,103–18,107, 1994.

Wernicke, B., G. J. Axen, and J. K. Snow, Basin and Range extensional tectonics at the latitude of Las Vegas, Nevada, *Geol. Soc. Am. Bull., 100,* 1738–1757, 1988.

Zhang, P. M., D. Ellis, D. Slemmons, and F. Mao, Right-lateral displacements and Holocene rate associated with prehistoric earthquakes along the southern Panamint Valley fault zone, *J. Geophys. Res., 95,* 4857–4872, 1990.

R. A. Bennett, J. L. Davis, P. Elósegui, Harvard-Smithsonian Center for Astrophysics, 60 Garden St, MS 42, Cambridge, MA, 02138 (e-mail: rbennett@cfa.harvard.edu)

B. P. Wernicke, J. K. Snow, M. J. Abolins, M. A. House, California Institute of Technology, Pasadena, CA, 91125

G. L. Stirewalt, D. A. Ferrill, Center for Nuclear Waste Regulatory Analyses, San Antonio, TX, 78238

(Received April 14, 1997; revised September 29, 1997; accepted October 3, 1997.)